Advances in Analytical Chemistry 2013, 3(3A): 9-13
DOI: 10.5923/s.aac.201307.02

Theory of Square-Wave Voltammetry for a Dissolved Redox Couple

Šebojka Komorsky-Lovrić, Milivoj Lovrić*

Department of Marine and Environmental Research, “Rudjer Bošković” Institute, P.O. Box 180, HR-10002 Zagreb, Hrvatska (Croatia)

Abstract A determination of the composition of dissolved mixture of reduced and oxidized forms of an electroactive compound by square-wave voltammetry is investigated theoretically. If electrode reaction is reversible, the sum of concentrations of these species can be measured by the standard addition method, while the ratio of their concentrations can be calculated from the ratio of the peak currents of the components of the response. If the transfer of electrons is kinetically controlled and the reduction and oxidation appear totally irreversible at the highest frequency, the concentrations of reactant and product may be measured separately.

Keywords Square-wave Voltammetry, Theory, Redox Couple

1. Introduction

In the analytical application of square-wave voltammetry it is usual that only the reactant of a certain electrode reaction is present in the solution initially[1 - 6]. However, in some cases both oxidized and reduced forms of the analyte may exist in the sample[7 - 10]. Some examples are solutions of anions and dianions of polysulfide[11], arsenite, arsenate[12, 13], iodide[14] and iodate ions[15, 16], compounds containing quinone and hydroquinone moieties [17, 18], various iron-based redox species[19, 20], peroxone [21], oxidized and reduced glutathione[22] and NADH/NAD$^+$ redox couple[23]. In the theory of square-wave voltammetry the presence of the product of electrode reaction was considered in the instances of reverse scan direction[24] and the use of equilibrium potential as the starting one[25]. In this paper the problem of speciation is addressed.

2. The Model

A simple electrode reaction is considered:

$$Ox^{m+} + ne^- \leftrightarrows Red^{(m-n)+} \qquad (1)$$

It is assumed that both the reactant Ox^{m+} and the product $Red^{(m-n)+}$ are soluble in the aqueous electrolyte and that they are initially present in the bulk of solution. Also, no convection is assumed. According to the first and the second Fick's laws, the mass transport towards the surface of stationary, planar electrode is described by the following differential equations:

$$\frac{\partial c_{ox}}{\partial t} = D\frac{\partial^2 c_{ox}}{\partial x^2} \qquad (2)$$

$$\frac{\partial c_{red}}{\partial t} = D\frac{\partial^2 c_{red}}{\partial x^2} \qquad (3)$$

The symbols c_{ox} and c_{red} stay for the concentrations of reactant and product, respectively, D is the common diffusion coefficient, t is time and x is the distance perpendicular to the electrode surface. The starting and the boundary conditions are the following:

$$t = 0, x \geq 0: \quad c_{ox} = c^*_{ox}, c_{red} = c^*_{red} \qquad (4)$$

$$t > 0, x \to \infty: c_{ox} \to c^*_{ox}, c_{red} \to c^*_{red} \qquad (5)$$

Here, c^*_{ox} and c^*_{red} are bulk concentrations of the reactant and product. The current depends on the flux of reactant at the electrode surface:

$$x = 0: \; D\left(\frac{\partial c_{ox}}{\partial x}\right)_{x=0} = -\frac{I}{nFS} \qquad (6)$$

$$D\left(\frac{\partial c_{red}}{\partial x}\right)_{x=0} = \frac{I}{nFS} \qquad (7)$$

The meanings of symbols are as follows: I is the current, n is the number of electrons, F is Faraday constant and S is the electrode surface area. Generally, the current depends on the standard rate constant (k_s), the transfer coefficient (α) and the dimensionless electrode potential (φ). This relationship is called Butler-Volmer equation:

$$\frac{I}{nFS} = -k_s\, Exp(-\propto \varphi)\, [(c_{ox})_{x=0} - (c_{red})_{x=0} Exp(\varphi)] \qquad (8)$$

$$\varphi = \frac{nF}{RT}(E - E^0) \qquad (9)$$

The symbols E, E^0, R and T stay for the electrode potential, the standard potential of the electrode reaction, the gas constant and the absolute temperature.

If the reaction (1) is fast and reversible, the Nernst equation applies instead of eq.(8):

---

* Corresponding author:
mlovric@irb.hr (Milivoj Lovrić)

$$(c_{ox})_{x=0} = (c_{red})_{x=0} \ \mathrm{Exp}(\varphi) \qquad (10)$$

Equations (2)– (9) are solved by digital simulation[26, 27]. A dimensionless diffusion coefficient and the time increment are defined as: $D\Delta t\Delta x^{-2} = 0.4$ and $\Delta t = (50f)^{-1}$, where Δx is the space increment and f is square-wave frequency. The solution is a dimensionless current: $\Phi = I(nFSc^{*}_{ox})^{-1}(Df)^{-½}$. A positive net response is defined as: $-\Delta\Phi = -(\Phi_f - \Phi_b)$, where Φ_f and Φ_b are forward and backward components of the response. Square-wave voltammetric excitation signal is defined by the pulse amplitude (E_{SW}), the scan increment (dE) and the starting potential (E_{st})[1-3]. The influences of low supporting electrolyte concentration, such as *IR* drop, migration and double layer effect on the charge transfer rate, are not considered. The calculations were performed by the Microsoft Quick Basic program.

3. Results and Discussion

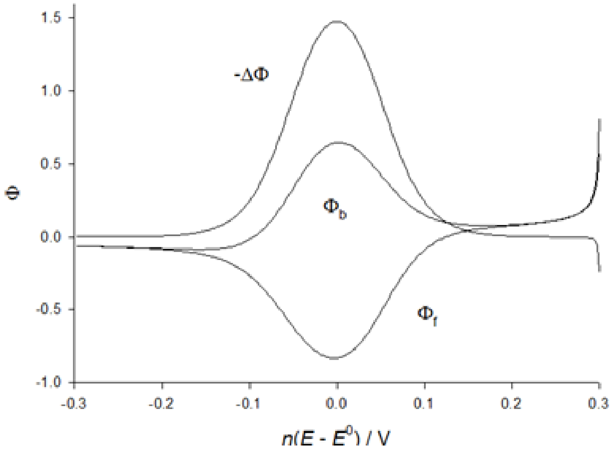

Figure 1. Theoretical square-wave voltammogram of reversible electrode reaction (1); $c^{*}_{ox} = c^{*}_{red}$, $E_{SW} = (50/n)$ mV, dE = -(2/n) mV and $E_{st} = (0.3/n)$ V *vs.* E^0. The dimensionless net response (-ΔΦ) and its forward (Φ_f) and backward (Φ_b) components are shown

Figure 1 shows square-wave voltammogram of reversible reaction (1) calculated for equal bulk concentrations of the reactant and product. The net response appears in the maximum at the standard potential and the potentials of minimum of the forward component and the maximum of backward component are -0.004 V and 0.002 V *vs.* E^0, respectively. If $E_{SW} = (50/n)$ mV, dE = -(2/n) mV and E_{st} = (0.3/n) V *vs.* E^0, the half-peak width of the net response is equal to (124/n) mV and the ratio of peak currents of the components is the following one: $I_{p,f} / I_{p,b} = -1.293$. These characteristics are independent of the square-wave frequency. The presence of the product in the bulk of the solution is indicated by the oxidation current appearing at the starting potential.

The dependence of dimensionless net peak current on the ratio of bulk concentrations of the product and the reactant is shown in Fig. 2A. The straight line is a linear approximation: $-\Delta\Phi_p = 0.7383 + 0.7383\ c^{*}_{red} / c^{*}_{ox}$. This means that the real net peak current depends linearly on the sum of bulk concentrations of the reactant and product: $-\Delta I_p = 0.7383\ nFS(Df)^{½}(c^{*}_{ox} + c^{*}_{red})$.

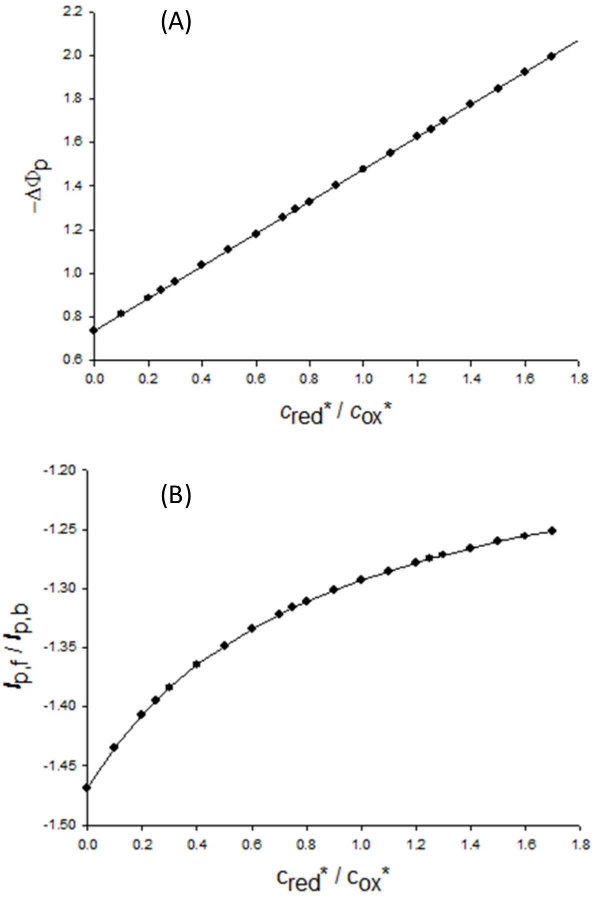

Figure 2. The dependence of dimensionless net peak current (A) and the ratio of peak currents of the forward and backward components (B) on the ratio of bulk concentrations of the product and the reactant. All data are as in Fig. 1

Table 1. A simulation of the standard addition method. Dependence of dimensionless peak currents of the forward and backward components, their ratio and the corresponding ratio of bulk concentrations of the product and the reactant (eq.12) on the dimensionless additions of the reactant to the sample

$\frac{(c^{*}_{ox})_{add}}{(c^{*}_{ox})_{init}}$	$\Phi_{p,f}^{*}$	$\Phi_{p,b}^{*}$	$\frac{I_{p,f}}{I_{p,b}}$	$\frac{c^{*}_{red}}{c^{*}_{ox}}$
0	-0.7154	0.5411	-1.3221	0.7
1	-1.1551	0.8404	-1.3745	0.35
2	-1.5948	1.1394	-1.3993	0.233
3	-2.0344	1.4391	-1.4137	0.175
4	-2.4741	1.7384	-1.4232	0.14
5	-2.9138	2.0377	-1.4300	0.117

Fig. 2B shows the relationship between the ratio of peak currents of the components and the ratio of bulk concentrations of the reduced and oxidized species. The best fitting curve is defined by the following equation:

$$\frac{I_{p,f}}{I_{p,b}} = -\left(1.2667 + 1.141\frac{c^{*}_{red}}{c^{*}_{ox}}\right)\left(0.8622 + \frac{c^{*}_{red}}{c^{*}_{ox}}\right)^{-1} \qquad (11)$$

Hence, the ratio c^{*}_{red} / c^{*}_{ox} can be calculated from experimentally measured ratio of peak currents of the components of the response using the inverse function:

$$\frac{c_{red}^{*}}{c_{ox}^{*}} = -\left(1.2667 + 0.8622\frac{I_{p,f}}{I_{p,b}}\right)\left(1.141 + \frac{I_{p,f}}{I_{p,b}}\right)^{-1} \quad (12)$$

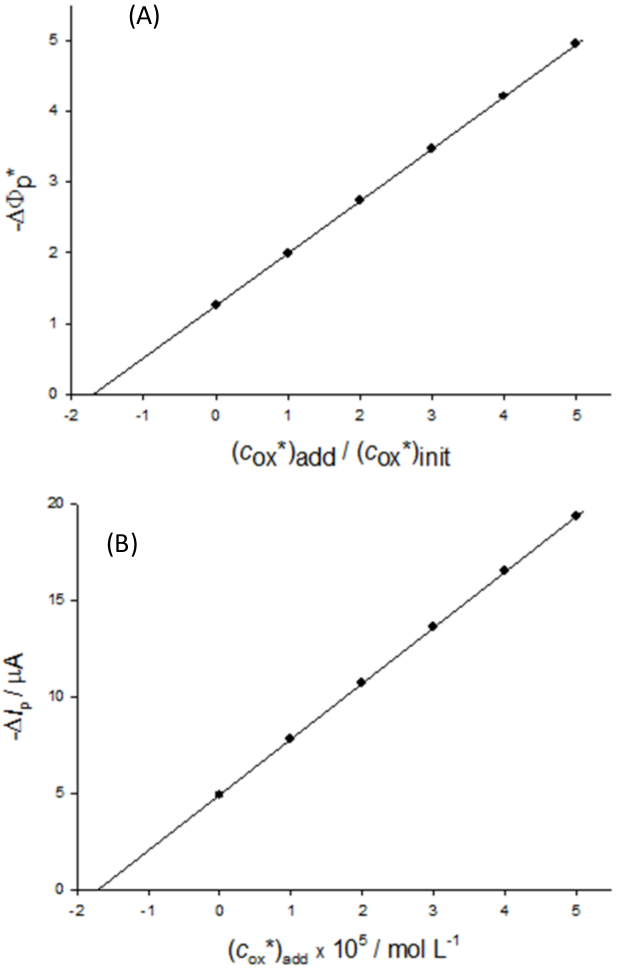

Figure 3. A simulation of the standard addition method. The dependence of dimensionless (A) and real (B) net peak current on the dimensionless (A) and real (B) concentration of reactant that is added to the sample. $(c^*_{ox})_{init}$ = 1×10^{-5} mol L^{-1}, $(c^*_{red})_{init}$ = 7×10^{-6} mol L^{-1}, $n = 1$, $F = 96485$ C mol^{-1}, $S = 0.1$ cm^2, $D = 9\times10^{-6}$ cm^2 s^{-1}, $f = 100$ s^{-1}, $E_{SW} = 50$ mV, dE = -2 mV and $E_{st} = 0.3$ V *vs.* E^0

In electroanalytical chemistry the influence of matrix can be compensated by the standard addition method in which the known amounts of analyte are added to the sample and measured. A theoretical example of this procedure is shown in Fig. 3 and Table 1. It is assumed that the sample contains both the reactant and product, with the ratio $(c^*_{red} / c^*_{ox})_{init} = 0.7$. The dimensionless currents are defined by the initial concentration of the reactant: $\Phi^* = I(nFS)^{-1}(c^*_{ox})_{init}^{-1}(Df)^{-1/2}$. It is further assumed that each addition of the reactant is equal to the initial concentration of the reactant in the sample. Fig. 3A shows the dependence of the dimensionless net peak current on the dimensionless concentration of the reactant for five additions. The straight line is a linear approximation: $-\Delta\Phi_p^* = 1.2550 + 0.7383(c^*_{ox})_{add} / (c^*_{ox})_{init}$. Its intersection with the axis $-\Delta\Phi_p^* = 0$ is defined by the equation: $(c^*_{ox})_{add} / (c^*_{ox})_{init} = -1.7$. The physical meaning of this number follows from the fact that the initial current $-\Delta\Phi_p^* = 1.2550$ is the consequence of the linear relationship $-\Delta\Phi_p^* = 0.7383\ (1 + (c^*_{red} / c^*_{ox})_{init})$. So, $(c^*_{ox} + c^*_{red})_{init} / (c^*_{ox})_{init} = 1.7$, as it is assumed. An example of real experiment, for arbitrarily chosen parameters, is shown in Fig. 3B. This shows that by the method of standard addition a total concentration of analyte, i.e. the sum of concentrations of its oxidized and reduced form, can be determined. The composition of this redox mixture can be estimated by means of the ratio of peak currents of the components of the response. This is shown in Table 1. In the imagined sample the ratio of peak currents is -1.3221 and for this value the result of eq.(12) is $c^*_{red} / c^*_{ox} = 0.7$, as it is assumed. After the first addition of the reactant its concentration is double and the ratio c^*_{red} / c^*_{ox} decreases to 0.35. This and the other results in Table 1 serve to control the accuracy of the first estimation.

Under the influence of kinetics of electrode reaction all characteristics of square-wave voltammogram depend on the frequency and the net response may split in two peaks[1, 3, 24]. For this reason eq.(12) does not apply to kinetically controlled electrode reactions. Also, the influence of the bulk concentration of product on the net peak current is diminished as the frequency is increased. For some quasi-reversible reactions the separation of responses of the reactant and product may be achieved at the highest frequency. Fig. 4 shows the transformation of voltammogram under the influence of dimensionless kinetic parameter $\kappa = \kappa_s(Df)^{-1/2}$. If $\kappa = 0.1$ and $c^*_{red} = c^*_{ox}$ the net peak potential is -0.030 V *vs.* E^0 and the potentials of extremes of components are -0.044 V and 0.018 V. Comparing to Fig. 1, the separation of maximum and minimum of the components is increased from 6 mV to 62 mV and the net peak current in Fig. 4A is 3.5 times smaller than in Fig. 1. This is mainly because the peak current of backward component is 7 times smaller in Fig. 4A than in Fig. 1. The ratio of peak currents of the components is -4 in Fig. 4A. If $\kappa = 0.01$, which can be achieved by the 100 times higher frequency, the response consists of two peaks. Their net peak potentials are -0.152 V and 0.184 V *vs.* E^0. They are caused by the separation of components: $E_{p,f}$= -0.159 V and $E_{p,b}$ = 0.238 V. The forward component corresponds to the reduction of reactant and the backward component corresponds to the oxidation of product. The later process is restricted by a deep diffusion layer of the product that is developed during the scan from 1 V to 0.3 V. One can note that the second peak appears as a difference between step-like changes of the forward and the backward components between 0.3 V and 0.1 V. This is, however, a minor component of the response that is dominated by the first peak. The reduction of reactant is totally irreversible process and the backward component in this potential range is also the reduction current. This means that the first net peak current under these conditions depends solely on the concentration of the reactant and only this concentration can be determined by the standard addition method. The concentration of the product in the bulk of solution can be measured by the inverse scan direction[24, 25].

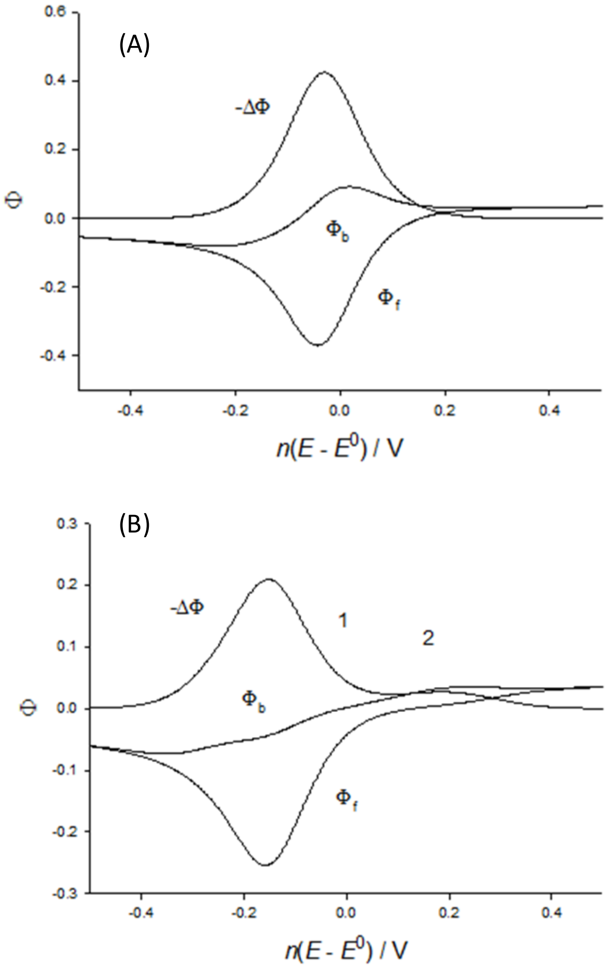

Figure 4. Theoretical square-wave voltammograms of electrode reaction (1) that is controlled by the charge transfer kinetics; $\kappa = 0.1$ (A) and 0.01 (B), $\alpha = 0.5$, $c^*_{ox} = c^*_{red}$, $nE_{SW} = 50$ mV, $ndE = -2$ mV and $nE_{st} = 1$ V *vs.* E^0

4. Conclusions

The linear relationship between the net peak current and the sum of concentrations of the reactant and product of reversible electrode reaction enables the determination of total content of an analyte in the sample. The ratio of concentrations of reduced and oxidized forms of this substance can be calculated from the ratio of peak currents of the forward and backward components of the response. If electrode reaction is controlled by the charge transfer kinetics, the reduction and oxidation processes may appear totally irreversible at the highest frequency. The net peak current of irreversible reduction depends only on the concentration of the reactant, which means that the redox composition of the analyte can be determined by separate measurements of the reactant and product concentrations.

REFERENCES

[1] V. Mirčeski, Š. Komorsky-Lovrić, M. Lovrić, Square-wave voltammetry, Springer, Berlin, 2007.

[2] J. Osteryoung, J. O'Dea, Square-wave voltammetry, in: A.J. Bard (Ed.), Electroanalytical Chemistry, Vol. 14, Marcel Dekker, New York, 1986, p. 209.

[3] J.J. O'Dea, J. Osteryoung, R.A. Osteryoung, Theory of square-wave voltammetry for kinetic systems, Anal. Chem. 53 (1981) 695.

[4] G.N. Eccles, Recent advances in pulse, cyclic and square-wave voltammetric analysis, Crit. Rev. Anal. Chem. 22 (1991) 345.

[5] R.A. Brookes, R.G. Compton, Simulation of square-wave voltammetry: quasi-reversible electrode processes, J. Phys. Chem. B 103 (1999) 9020.

[6] D. de Souza, L. Codognoto, A.R. Malagutti, R.A. Toledo, V.A. Pedroso, T.R.S. Oliverira, L.H. Mazo, L.A. Avaca, S.A.S. Machado, Square-wave voltammetry. Second part: applications, Quim. Nova 27 (2004) 790.

[7] A. Demortier, C. Jehoulet, Digital simulation of cyclic voltammetric curves when the oxidized and the reduced form of a redox couple are present in solution, J. Electroanal. Chem. 283 (1990) 15.

[8] J.W. Weidner, P.S. Fedkiw, Reversible linear-sweep voltammetry of a soluble redox couple: effect of initial concentrations, Anal. Chem. 62 (1990) 875.

[9] A.M. Keitghtley, J.C. Myland, K.B. Oldham, P.G. Symons, Reversible cyclic voltammetry in the presence of product, J. Electroanal. Chem. 322 (1992) 25.

[10] C. Serna, A. Molina, General solutions for the I-t response for reversible processes in the presence of product in a multipotential step experiment at planar and spherical electrode whose areas increase with any power of time, J. Electroanal. Chem. 466 (1999) 8.

[11] E. Levillain, F. Gaillard, J.P. Lelieur, Polysulfides in dimethylformamide: only the redox couples Sn^-/Sn^{2-} are involved, J. Electroanal. Chem. 440 (1997) 243.

[12] U. Yogeswaran, M.S. Chen, S.H. Li, Electroanalytical responses of arsenic oxide, methanol and oxygen at the ruthenium oxide hexachloroiridate with platinum hybrid film, Electroanalysis 20 (2008) 2324.

[13] R. van Lis, W. Nitschke, S. Duval, B. Schoepp-Cothenet, Arsenics as bioenergetic substrates, Biochim. Biophys. Acta – Bioenerg. 1827 (2013) 176.

[14] S. Fierro, C. Comninellis, Y. Einaga, Simultaneous detection of iodine and iodide on boron doped diamond electrodes, Talanta 103 (2013) 33.

[15] V. Žic, V.W. Truesdale, N. Cukrov, The distribution of iodide and iodate in anchialine cave waters. Evidence for sustained localized oxidation of iodide to iodate in marine water, Marine Chem. 112 (2008) 168.

[16] K. Bluhm, P. Croot, K. Wuttig, K. Lochte, Transformation of iodate to iodide in marine phytoplankton driven by cell senescence, Aquat. Biol. 11 (2010) 1.

[17] P.S. Guin, S. Das, P.C. Mandal, Electrochemical reduction of quinones in different media: a review, Int. J. Electrochem. (2011) Ms ID 816202.

[18] M.A. Bhat, Mechanistic, kinetic and electroanalytical aspects of quinone-hydroquinone redox system in N-alkylimidazolium based room temperature ionic liquids, Electrochim. Acta 81 (2012) 275.

[19] G. Battistuzzi, M. Bellei, C.A. Bortolotti, M. Sola, Redox properties of heme peroxidases, Arch. Biochem. Biophys. 500 (2010) 21.

[20] O. Scialdone, C. Guarisco, S. Crispo, A. D'Angelo, A. Galia, Investigation of electrode material. Redox couple systems for reverse electrodialysis processes. Part I: iron redox couples, J. Electroanal. Chem. 681 (2012) 66.

[21] M.I. Awad, T. Ohsaka, Electroanalysis of peroxone, Electrochem. Commun. 6 (2004) 1135.

[22] R. Kizek, J. Vacek, L. Trnkova, F. Jelen, Cyclic voltammetric study of the redox system of glutathione using the disulfide bond reductant tris(2-carboxyethyl)phosphine, Bioelectrochem. 63 (2004) 19.

[23] F.S. Saleh, M.R. Rahman, T. Okajima, L. Mao, T. Ohsaka, Determination of formal potential of NADH/NAD$^+$ redox couple and catalytic oxidation of NADH using poly(phenosafranin)-modified carbon electrodes, Bioelectrochem. 80 (2011) 121.

[24] Š. Komorsky-Lovrić, M. Lovrić, Square-wave voltammetry of dissolved redox couple, Russ. J. Electrochem. 46 (2010) 1373.

[25] D. Jadreško, Theory of square-wave voltammogram starting at the equilibrium potential, J. Electroanal. Chem. 693 (2013) 56.

[26] S.W. Feldberg, Digital simulation: a general method for solving electrochemical diffusion – kinetic problems, in: A.J. Bard (Ed.), Electroanalytical Chemistry, Vol. 3, Marcel Dekker, New York, 1969, p. 199.

[27] B. Speiser, Numerical simulation of electroanalytical experiments: recent advances in methodology, in A.J. Bard (Ed.), Electroanalytical Chemistry, Vol 19, Marcel Dekker, New York, 1996, p. 2.